BIOCHEMISTRY
including biophysical chemistry & molecular biology

Article

pubs.acs.org/biochemistry

DNA Base Pair Hybridization and Water-Mediated Metastable Structures Studied by Molecular Dynamics Simulations

Wenpeng Qi,[†,‡] Bo Song,*[,†] Xiaoling Lei,[†] Chunlei Wang,[†] and Haiping Fang*[,†]

[†]Shanghai Institute of Applied Physics, Chinese Academy of Sciences, P.O. Box 800-204, Shanghai 201800, China

[‡]Department of Physics, Shandong University, Jinan, Shandong 250100, China

Supporting Information

ABSTRACT: The base pair hybridization of a DNA segment was studied using molecular dynamics simulation. The results show the obvious correlation between the probability of successful hybridization and the accessible surface area to water of two successive base pairs, including the unpaired base pair adjacent to paired base pair and this adjacent paired base pair. Importantly, two metastable structures in an A−T base pair were discovered by the analysis of the free energy landscape. Both structures involved addition of a water molecule to the linkage between the two nucleobases in one base pair. The existence of the metastable structures provide potential barriers to the Watson−Crick base pair, and numerical simulations show that those potential barriers can be surmounted by thermal fluctuations at higher temperatures. These studies contribute an important step toward the understanding of the mechanism in DNA hybridization, particularly the effect of temperature on DNA hybridization and polymerase chain reaction. These observations are expected to be helpful for facilitating experimental bio/nanotechnology designs involving fast hybridization.

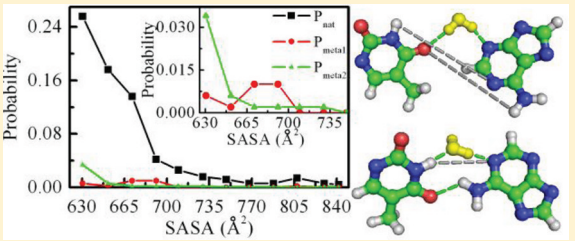

DNA hybridization plays a central role in molecular biology and in the formation of bio-related materials and techniques used in biotechnology, such as the polymerase chain reaction, DNA sequencing, and DNA detection.[1−5] Since single-stranded DNA uniquely recognizes its complementary strand, novel molecular devices on the nanoscale, such as nanotriggers and DNA specified nanotransporters, are possible.

Based on the first study by Wetmur and Davidson performed in 1968,[6] many theoretical models have been proposed for describing the kinetics of DNA hybridization.[7,8] In the past two decades, molecular dynamics (MD) simulations have been used extensively into the study of biomolecules.[9−18] With the help of MD simulations, the dehybridization process of one DNA base pair[19,20] and DNA/RNA hairpin folding[21,22] have been studied. Experimentally, DNA hybridization has also been investigated.[23−29] Zhao et al. recently found that DNA hybridization showed non-Arrhenius behavior.[23] Despite the efforts, the mechanism of DNA hybridization is still far from being fully understood.

We present a study toward the base pair hybridization of DNA by MD simulations. We found that the probability of successful hybridization depends significantly on the initial structures of the unpaired DNA. Two of the structures in an A−T base pair involved the addition of a water molecule to the linkage between the two nucleobases. Those metastable structures provide potential barriers to the Watson−Crick base pair and numerical simulations show that those potential barriers can be surmounted by thermal fluctuations at higher temperatures. To our knowledge, this is the first report to these metastable structures at the room temperature and their impact on hybridization. The presented simulations contribute an important step toward our understanding of the mechanism and the physics in DNA hybridization and hybridization-related processes, such as the polymerase chain reaction.

MATERIALS AND SIMULATIONS

To prepare the initial conformations, we first performed an MD simulation at 530 K for 20 ns for a DNA segment of poly(dA)$_6$−poly(dT)$_6$, in which the first three base pairs are constrained in the form of Watson−Crick base pair. Since this temperature is much higher than the melting temperature of DNA, the other three base pairs become unpaired during the simulation as the typical example shown in Figure 1a. The structure of the Watson−Crick base pair[30] is shown in Figure 1b, together with the designation of the atoms. Namely, the Watson−Crick structure of A−T base pair in our simulations is defined as the formation of both hydrogen bonds (dT)N3−H···N1(dA) and (dT)O4···H−N6(dA). The initial conformations were selected from the snapshots during the simulation, according to the solvent accessible surface area (SASA) of the first unpaired base pair (BP1) adjacent to paired base pair and this adjacent paired base pair (BP0). SASA is defined as the surface area of the two neighboring base pairs accessible to a water molecule[31] as represented by the two examples presented in Figure 1c,d. SASA has a minimal value about 540 Å^2 when both BP0 and BP1 form Watson−Crick base pairs. Numeri-

Received: February 22, 2011
Revised: October 6, 2011
Published: October 10, 2011

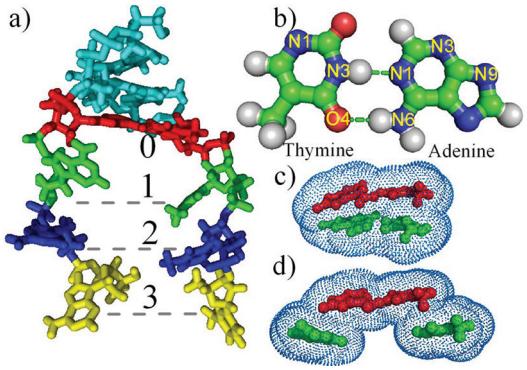

Figure 1. (a) Typical initial conformation of the DNA segment. The three unpaired base pairs are indexed by 1 (green), 2 (blue), and 3 (yellow), and the Watson–Crick base pair adjacent to the unpaired base pair 1 is indicated by 0 (red). (b) A Watson–Crick A–T base pair and the designation of atoms. (c, d) Schematic representations of the solvent accessible surface area (SASA) of the base pair 0 and the base pair 1 with a well-paired (c) and an unpaired (d) structure, indicated by the cloud surface around the two base pairs. The SASA of 733 Å^2 in the unpaired structure is significantly larger than the SASA of 570 Å^2 in the paired structure.

cally, we found the maximal value of SASA was 860 Å^2. We divided the interval from 620 to 860 Å^2 into 12 subintervals and selected 50 different conformations randomly in each subinterval to obtain 600 initial conformations.

The initial DNA segment was immersed in a periodic box of 4.0 nm × 4.0 nm × 4.0 nm. There are 1978 TIP3P water molecules[32] in the water box. Ten Na^+ ions were added to neutralize the whole system. All MD simulations were performed via Gromacs 4.0[33] with the Amber03 force field.[34] A cutoff of 1 nm was applied for the Lennard-Jones interaction and the real space portion of the electrostatic interaction, while the PME method was used for the reciprocal space portion of the electrostatic interaction.[35] For each conformation, the whole system was first equilibrated for 1 ns under NPT conditions, a constant pressure of 1 bar and a temperature of 298 K, with all the DNA and ions position restrained, then 10 different velocity distributions were sampled according to the simulation temperature by a Maxwell distribution, and a 5 ns NVT MD simulation was performed with the three paired base pairs constrained at 298 K. The Nose–Hoover[36] thermostat was used for temperature coupling, and the Parrinello–Rahman[37] pressure-stat was used for pressure coupling. The total simulation time is more than 30 μs.

RESULTS AND DISCUSSION

The solid squares in Figure 2 show the probability for the successful hybridization of the first unpaired base pair, BP1, denoted by P_{nat}, with respect to the initial conformations (characterized by SASA). P_{nat} is defined as the ratio of the number of successful hybridized simulations to the whole number of performed simulations in each subinterval of the SASA. Successful hybridization was defined as the appearance of the Watson–Crick base pair more than 75% of the time in the final 4 ns for each simulation. We found that P_{nat} decreased as the SASA increased, indicating that the hybridization significantly depends on the initial conformations. P_{nat} showed a relative fast decreasing for 620 Å^2 < SASA < 690 Å^2. The hybridization probability is very small between 720 and 850 Å^2.

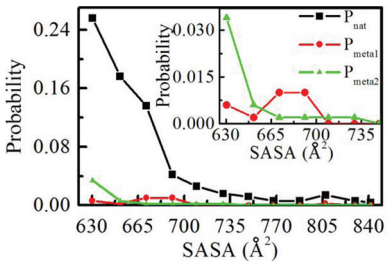

Figure 2. Probabilities for the successful hybridization, P_{nat} (■, black solid curve), the metastable structure 1, P_{meta1} (●, red solid curve), and metastable structure 2, P_{meta2} (▲, green solid curve), of the base pair 1, with respect to the solvent accessible surface area (SASA). The inset is the zoom-in for P_{meta1} and P_{meta2}.

We note that the SASA of the two successive base pairs describes the stacking geometry of the bases. The stacking geometry determines the base stacking interaction between two neighboring bases.[38] The base stacking interaction is the main reason for stabilizing the DNA structures.[39] Figure 1 shows that the hybridization probabilities correlate well with the SASA of the two successive base pairs, which suggests that the stacking interaction plays a role on the hybridization process obviously. The SASA can describe the stacking geometry, but it has an obvious shortcoming that different molecular conformations will give the same SASA. Here we use another parameter l, the distance between the atom N3 in the thymine and N1 in the adenine of BP1, combined with the SASA of BP0 and BP1 to describe the hybridization free energy difference, as shown in Figure 3.

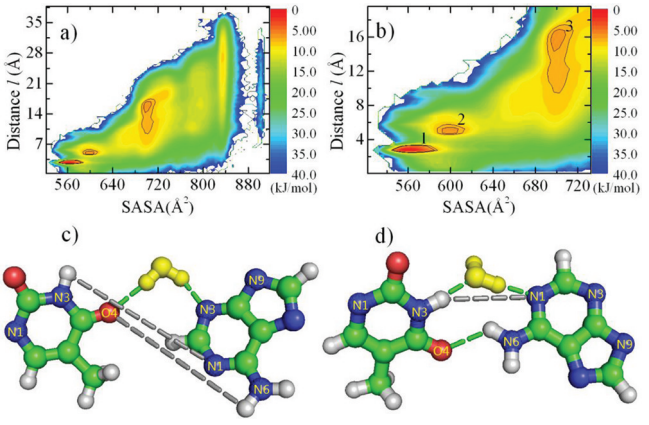

Figure 3. (a) Hybridization free energy differences of DNA base pair versus two reaction coordinates the distance l (between the atom N3 in the thymine and the atom N1 in the adenine of BP1) and the SASA (BP0 and BP1). (b) The zoom-in of the free energy landscape around the three energy minima. The two contour lines correspond to the free energies of 9 and 10 kJ/mol. The numbers 1, 2, and 3 stand for the local minima found in the free energy landscape. The minimum 1 corresponds to the Watson–Crick base pair structure. The minimum 2 corresponds to two metastable structures, as shown in (c) and (d). The minimum 3 corresponds to a kind of dehybridized structures. (c) The metastable structure 1. (d) The metastable structure 2. The water molecules are colored yellow. The green dashed lines indicate hydrogen bonds. The gray dashed lines in (c, d) serve as a guide only and correspond to the hydrogen bonds in the Watson–Crick base pair.

The free energy difference $F = -RT \ln(P_{l,S})$, where $P_{l,S}$ is the fraction of structures with the distance l (between the atom N3

dx.doi.org/10.1021/bi2002778 | Biochemistry 2011, 50, 9628–9632

in the thymine and the atom N1 in the adenine) and the solvent accessible surface area S (of BP1 and BP0). The reference state is the Watson−Crick base pair structure. From Figure 3 we can distinguish three minima by the two black contour lines that correspond to the free energies of 9 and 10 kJ/mol, respectively. In Figure 3b, the minimum 1 ($l \approx 3.0$ Å and 540 Å^2 < SASA < 590 Å^2) corresponds to the Watson−Crick base pair structure. The minimum 2 (5.0 Å < l < 6.0 Å and 580 Å^2 < SASA < 620 Å^2) corresponds to two metastable structures, as shown in Figure 3c,d. The minimum 3 (15.0 Å < l < 17.0 Å and 680 Å^2 < SASA < 700 Å^2) corresponds to a kind of dehybridized structure that one base of BP1 is collapsed on the BP0, while the other base leaves away. Two typical structures of the minimum 3 are shown in the Supporting Information in Figure S1a,b, in which the two bases of BP1 in these structures neither form hydrogen bonds directly nor be connected by water molecules

After careful examination of the structures in the minimum 2, only Meta1 and Meta2 were found to maintain more than 3 ns. Comparing Meta1 with the Watson−Crick base pair, we observe the atom N3 of the thymine has moved toward the minor groove, and the atom N1 of the adenine has moved toward the major groove (Figure 3c). Both hydrogen bonds presenting in the Watson−Crick base pair were disrupted in Meta1. The new structure was stabilized by the formation of a water bridge [(dT)O4···H−O−H···N3(dA)], in which the atom O4 of the thymine and the atom N3 of the adenine formed hydrogen bonds with one water molecule simultaneously. We note that the two bases in Meta1 were not directly connected. For Meta2, the hydrogen bond between the atom N3 of the thymine and the atom N1 of the adenine existing in the Watson−Crick base pair was broken, and a water molecule was sandwiched between these bases to form a hydrogen-bond bridge of [(dT)N3−H···O−H(water)···N1(dA)] (Figure 3d). The second hydrogen bond presenting in the Watson−Crick base pair, between the atom O4 of the thymine and the atom N6 of the adenine, remained intact. Some different water bridged structures had been found by Giudice et al.[40] and Bouvier et al.[41] in the base pair opening process.

There are variations of the glycosidic torsion angles in both adenine and thymine in Meta1 and Meta2. The distributions of the glycosidic torsion angles in the two metastable structures are provided in the Supporting Information, Figure S2.

We also computed the probabilities for the appearance of Meta1 and Meta2 denoted by P_{meta1} and P_{meta2}, respectively (Figure 2). Here we defined the appearance of a metastable structure in each simulation as when the structure appears more than 75% of the time in the final 4 ns of the simulation. Meta1 mainly appeared at about 675 Å^2, whereas Meta2 mainly appeared at 630 Å^2. We have also studied the effect of the temperature on the metastable structures by performing 5 ns MD simulations at a high temperature 320 K, starting from the 10 metastable structures of Meta1 and Meta2 obtained at 298 K, respectively. During these high-temperature simulations, six Watson−Crick base pairs formed from the Meta1 structures, whereas three base pairs became unpaired and only one remained as Meta1. For Meta2, eight structures formed a Watson−Crick base pair, whereas the other two structures became unpaired. This indicates that the potential barriers to the Watson−Crick base pair due to the metastable structures can be surmounted by thermal fluctuations at higher temperatures. We note that Zhao et al. found static disorders at temperatures lower than 313 K,[23] and Ma et al. showed that a temperature-dependent phase was present in RNA hairpin folding.[24] Nikolova et al. presented NMR evidence for spontaneous loss of Watson−Crick pairing in canonical double helices.[42] The existence of the metastable structures together with its temperature-dependence behavior is helpful to the understanding of those experimental observations.

The total probabilities of forming the metastable structures and the Watson−Crick base pair structure in BP1 were 0.6% and 5.8% at 298 K (Figure 2), respectively. From the simulations at 320 K, we observed most of metastable structures becoming the Watson−Crick base pair structure. This suggests that P_{nat} at the low temperature reduced about 0.6% with respect to the case at the high temperature, which is 0.006/(0.006 + 0.058) = 9.4% in the expectable successful hybridization events. For a long DNA molecule with 30 base pairs, the probability of the metastable-structure blockage is about $1 - (1 - 9.4\%)^{30} \approx 95\%$, which means that 95% of expected successful hybridization events at the high temperature are blocked at the low temperature by the metastable structures. Therefore, the metastable structures greatly reduce the hybridization probability in long DNA molecules at room temperature.

We have also investigated the hybridization of the second and third unpaired base pairs from the simulation data. The probability was only 0.57% for the successful hybridization of both the first and the second base pairs. This value is significantly smaller than the probabilities of successful hybridization of the first base pair (i.e., 5.8%). We found only two successful hybridization cases for all three base pairs in the 6000 simulations. We have estimated the hybridization time τ of 3 base pairs using the method mentioned in the article of Sorin et al.[21] The hybridization time τ is about 14 ± 1.5 μs, which is in agreement with folding times of ∼10 μs reported for nucleic acid hairpins in both experiment[27] and simulation[21] results. This shows that the hybridization of the initial random conformations of the unpaired segments has a very low probability for long sequences. We note that the metastable structures Meta1 and Meta2 were also observed for the second unpaired base pair, revealing that the occurrence of the metastable structures is universal.

The probabilities of successful hybridization are the results of 5 ns simulaiton. If we perform longer simulations, the values of these probabilities may be varied. However, the decreasing tendency in Figure 2, the hybridization time τ, and the free energy landscape in Figure 3 will be remained because we have sampled the phase space of DNA conformation by a huge number of initial structures and different initial velocity distributions.

It has been argued that slide action plays an important role in the hybridization of DNA with repetitive sequences.[43,44] We have also observed some slide action cases. However, the base-to-base hybridization dominates in our simulations. This is partly because a short DNA segment was taken in our investigation; i.e., here we focused on the hybridization process of the three base pairs which were adjacent to the other three constrained base pairs in the form of Watson−Crick base pairs in the simulations. For longer DNA segments without those constrained base pairs, the sliding action may play a more significant role. Perez et al. found a minor error in the backbone parameters of the Amber force fields. Thus, the overpopulation of the (α, γ) = (g+, t) backbone conformations were observed in single long (more than 10 ns) simulations.[45] In our 5 ns single simulation, this effect is not observable. A modified

version[45] will be used in our next studies where much longer simulations will be performed benifited from the development of computers.

We have found that the probability of successful hybridization decreased as the solvent accessible surface area of two successive base pairs increased. Importantly, two metastable structures were discovered by the analysis of the free energy landscape of an A−T base pair. Both structures involved the addition of a water molecule to the linkage between the two nucleobases in one base pair. We noted that to our knowledge this is the first report to describe Meta1. Although Meta2 has been previously predicted by ab initio calculations at zero temperature,[46] our simulation results reveal the remarkable observation that this structure still exists at room temperature. The simulations presented contribute an important step toward our understanding of the mechanism and the physics involved in DNA hybridization and hybridization-related process, such as the polymerase chain reaction. These studies may be also helpful to the facilitation of the experimental designs for fast hybridization, a process that is believed to be very important in bio/nanotechnology.

■ ASSOCIATED CONTENT

Ⓢ Supporting Information

Typical structures in the minimum 3 on the free energy landscape in Figure 3a,b, the glycosidic torsion variations in Meta1 and Meta2, the result of P_{nat} by the bootstrap method, and some detailed simulation paramters. This material is available free of charge via the Internet at http://pubs.acs.org.

■ AUTHOR INFORMATION

Corresponding Author

*E-mail: fanghaiping@sinap.ac.cn (H.F.), bosong@sinap.ac.cn (B.S.). Tel: -86-021-59554785. Fax: 86-21-39192394.

Funding

This work was supported by NNSFC (10825520), NBRPC (2007CB936000 and 2010CB934504), KIPCAS, the International office of BMBF Germany (CHN 08/028), and the Shanghai Supercomputer Center of China.

■ ABBREVIATIONS

MD, molecular dynamics; SASA, solvent accessible surface area; BP, base pair.

■ REFERENCES

(1) Bloomfield, V. A. (2000) *Nucleic Acids: Structure, Properties and Functions*, Stiefe, J., Ed., Sausalito, CA.

(2) Cao, Y. W. C., Jin, R. C., and Mirkin, C. A. (2002) Nanoparticles with Raman spectroscopic fingerprints for DNA and RNA detection. *Science 297*, 1536−1540.

(3) Saiki, R. K., Gelfand, D. H., Stoffel, S., Scharf, S. J., Higuchi, R., Horn, G. T., Mullis, K. B., and Erlich, H. A. (1988) Primer-directed enzymatic amplification of DNA with a thermostable DNA-polymerase. *Science 239*, 487−491.

(4) Keyser, U. F., Koeleman, B. N., Van Dorp, S., Krapf, D., Smeets, R. M. M., Lemay, S. G., Dekker, N. H., and Dekker, C. (2006) Direct force measurements on DNA in a solid-state nanopore. *Nature Phys. 2*, 473−477.

(5) Song, B., Elstner, M., and Cuniberti, G. (2008) Anomalous Conductance Response of DNA Wires under Stretching. *Nano Lett. 8*, 3217−3220.

(6) Wetmur, J. G., and Davidson, N. (1968) Kinetics of renaturation of DNA. *J. Mol. Biol. 31*, 349−&.

(7) Sikorav, J.-L., Orland, H., and Braslau, A. (2009) Mechanism of Thermal Renaturation and Hybridization of Nucleic Acids: Kramers' Process and Universality in Watson-Crick Base Pairing. *J. Phys. Chem. B 113*, 3715−3725.

(8) Ouldridge, T. E., Louis, A. A., Doye, J. P. K. DNA Nanotweezers Studied with a Coarse-Grained Model of DNA, *Phys. Rev. Lett. 104*, 178101.

(9) Zhou, R. H., Huang, X. H., Margulis, C. J., and Berne, B. J. (2004) Hydrophobic collapse in multidomain protein folding. *Science 305*, 1605−1609.

(10) Tajkhorshid, E., Nollert, P., Jensen, M. O., Miercke, L. J. W., O'Connell, J., Stroud, R. M., and Schulten, K. (2002) Control of the selectivity of the aquaporin water channel family by global orientational tuning. *Science 296*, 525−530.

(11) Kim, Y. C., Tang, C., Clore, G. M., and Hummer, G. (2008) Replica exchange simulations of transient encounter complexes in protein-protein association. *Proc. Natl. Acad. Sci. U. S. A. 105*, 12855−12860.

(12) Li, J. Y., Gong, X. J., Lu, H. J., Li, D., Fang, H. P., and Zhou, R. H. (2007) Electrostatic gating of a nanometer water channel. *Proc. Natl. Acad. Sci. U. S. A. 104*, 3687−3692.

(13) Gu, W., and Helms, V. (2009) Tightly Connected Water Wires Facilitate Fast Proton Uptake at The Proton Entrance of Proton Pumping Proteins. *J. Am. Chem. Soc. 131*, 2080−+.

(14) Gong, X. J., Li, J. Y., Lu, H. J., Wan, R. Z., Li, J. C., Hu, J., and Fang, H. P. (2007) A charge-driven molecular water pump. *Nature Nanotechnol. 2*, 709−712.

(15) Wang, C. L., Lu, H. J., Wang, Z. G., Xiu, P., Zhou, B., Zuo, G. H., Wan, R. Z., Hu, J. Z., and Fang, H. P. (2009) Stable Liquid Water Droplet on a Water Monolayer Formed at Room Temperature on Ionic Model Substrates. *Phys. Rev. Lett. 103*, 137801.

(16) Krone, M. G., Hua, L., Soto, P., Zhou, R. H., Berne, B. J., and Shea, J. E. (2008) Role of water in mediating the assembly of Alzheimer amyloid-β Aβ16−22 protofilaments. *J. Am. Chem. Soc. 130*, 11066−11072.

(17) McCullagh, M., Zhang, L., Karaba, A. H., Zhu, H., Schatz, G. C., and Lewis, F. D. (2008) Effect of loop distortion on the stability and structural dynamics of DNA hairpin and dumbbell conjugates. *J. Phys. Chem. B 112*, 11415−11421.

(18) Ma, H. R., Wan, C. Z., Wu, A. G., and Zewail, A. H. (2007) DNA folding and melting observed in real time redefine the energy landscape. *Proc. Natl. Acad. Sci. U. S. A. 104*, 712−716.

(19) Hagan, M. F., Dinner, A. R., Chandler, D., and Chakraborty, A. K. (2003) Atomistic understanding of kinetic pathways for single base-pair binding and unbinding in DNA. *Proc. Natl. Acad. Sci. U. S. A. 100*, 13922−13927.

(20) Stofer, E., Chipot, C., and Lavery, R. (1999) Free Energy Calculations of Watson-Crick Base Pairing in Aqueous Solution. *J. Am. Chem. Soc. 121*, 9503−9508.

(21) Sorin, E. J., Rhee, Y. M., and Pande, V. S. (2005) Does water play a structural role in the folding of small nucleic acids? *Biophys. J. 88*, 2516−2524.

(22) Garcia, A. E., and Paschek, D. (2008) Simulation of the pressure and temperature folding/unfolding equilibrium of a small RNA hairpin. *J. Am. Chem. Soc. 130*, 815−+.

(23) Chen, X., Zhou, Y., Qu, P., and Zhao, X. S. (2008) Base-by-Base Dynamics in DNA Hybridization Probed by Fluorescence Correlation Spectroscopy. *J. Am. Chem. Soc. 130*, 16947−16952.

(24) Ma, H. R., Proctor, D. J., Kierzek, E., Kierzek, R., Bevilacqua, P. C., and Gruebele, M. (2006) Exploring the energy landscape of a small RNA hairpin. *J. Am. Chem. Soc. 128*, 1523−1530.

(25) Goldar, A., and Sikorav, J. L. (2004) DNA renaturation at the water-phenol interface. *Eur. Phys. J. E 14*, 211−239.

(26) Chaperon, I., and Sikorav, J. L. (1998) Renaturation of condensed DNA studied through a decoupling scheme. *Biopolymers 46*, 195−200.

(27) Ansari, A., Kuznetsov, S. V., and Shen, Y. (2001) Configurational diffusion down a folding funnel describes the dynamics of DNA hairpins. *Proc. Natl. Acad. Sci. U. S. A. 98*, 7771−7776.

(28) Altan-Bonnet, G., Libchaber, A., and Krichevsky, O. (2003) Bubble dynamics in double-stranded DNA. *Phys. Rev. Lett. 90*, 138101.
(29) Jung, J. Y., and Van Orden, A. (2006) A three-state mechanism for DNA hairpin folding characterized by multiparameter fluorescence fluctuation spectroscopy. *J. Am. Chem. Soc. 128*, 1240−1249.
(30) Watson, J. D., and Crick, F. H. C. (1953) Molecular structure of nucleic acids - a structure for deoxyribose nucleic acid. *Nature 171*, 737−738.
(31) Lee, B., and Richards, F. M. (1971) Interpretation of protein structures - estimation of static accessibility. *J. Mol. Biol. 55*, 379.
(32) Jorgensen, W. L., Chandrasekhar, J., Madura, J. D., Impey, R. W., and Klein, M. L. (1983) Comparison of simple potential functions for simulating liquid water. *J. Chem. Phys. 79*, 926−935.
(33) Hess, B., Kutzner, C., van der Spoel, D., and Lindahl, E. (2008) GROMACS 4; Algorithms for Highly Efficient, Load-Balanced, and Scalable Molecular Simulation. *J. Chem. Theory Comput. 4*, 435−447.
(34) Sorin, E. J., and Pande, V. S. (2005) Exploring the Helix-Coil Transition via All-Atom Equilibrium Ensemble Simulations. *Biophys. J. 88*, 2472−2493.
(35) Darden, T., York, D., and Pedersen, L. (1993) Particle mesh Ewald: An N• log(N) method for Ewald sums in large systems. *J. Chem. Phys. 98*, 10089−10092.
(36) Nose, S. (1984) A unified formulation of the constant temperature molecular-dynamics methods. *J. Chem. Phys. 81*, 511−519.
(37) Parrinello, M., and Rahman, A. (1981) Polymorphic transitions in single-crystals - a new molecular-dynamics method. *J. Appl. Phys. 52*, 7182−7190.
(38) Sponer, J., Leszczynski, J., and Hobza, P. (1996) Nature of nucleic acid-base stacking: Nonempirical ab initio and empirical potential characterization of 10 stacked base dimers. Comparison of stacked and H-bonded base pairs. *J. Phys. Chem. 100*, 5590−5596.
(39) Sponer, J., Riley, K. E., and Hobza, P. (2008) Nature and magnitude of aromatic stacking of nucleic acid bases. *Phys. Chem. Chem. Phys. 10*, 2595−2610.
(40) Giudice, E., Varnai, P., and Lavery, R. (2003) Base pair opening within B-DNA: free energy pathways for GC and AT pairs from umbrella sampling simulations. *Nucleic Acids Res. 31*, 1434−1443.
(41) Bouvier, B., and Grubmuller, H. (2007) Molecular dynamics study of slow base flipping in DNA using conformational flooding. *Biophys. J. 93*, 770−786.
(42) Nikolova, E. N., Kim, E., Wise, A. A., O'Brien, P. J., Andricioaei, I., and Al-Hashimi, H. M. (2011) Transient Hoogsteen base pairs in canonical duplex DNA. *Nature 470*, 498−502.
(43) Sambriski, E. J., Schwartz, D. C., and de Pablo, J. J. (2009) Uncovering pathways in DNA oligonucleotide hybridization via transition state analysis. *Proc. Natl. Acad. Sci. U. S. A. 106*, 18125−18130.
(44) Kannan, S., and Zacharias, M. (2009) Simulation of DNA double-strand dissociation and formation during replica-exchange molecular dynamics simulations. *Phys. Chem. Chem. Phys. 11*, 10589−10595.
(45) Perez, A., Marchan, I., Svozil, D., Sponer, J., Cheatham III, T. E., Laughton, C. A., Orozco, M. Refinement of the AMBER Force Field for Nucleic Acids: Improving the Description of α/γ Conformers, *Biophys. J. 92*, 3817−3829.
(46) Kryachko, E. S., and Volkov, S. N. (2001) Preopening of the DNA base pairs. *Int. J. Quantum Chem. 82*, 193−204.